

Multi-fingered Robotic Hand Grasping in Cluttered Environments through Hand-Object Contact Semantic Mapping

Lei Zhang^{1,2}, Kaixin Bai^{1,2†}, Guowen Huang^{2,3}, Zhenshan Bing³,
Zhaopeng Chen², Alois Knoll³, Jianwei Zhang¹

Abstract—The deep learning models has significantly advanced dexterous manipulation techniques for multi-fingered hand grasping. However, the contact information-guided grasping in cluttered environments remains largely underexplored. To address this gap, we have developed a method for generating multi-fingered hand grasp samples in cluttered settings through contact semantic map. We introduce a contact semantic conditional variational autoencoder network (CoSe-CVAE) for creating comprehensive contact semantic map from object point cloud. We utilize grasp detection method to estimate hand grasp poses from the contact semantic map. Finally, an unified grasp evaluation model is designed to assess grasp quality and collision probability, substantially improving the reliability of identifying optimal grasps in cluttered scenarios. Our grasp generation method has demonstrated remarkable success, outperforming state-of-the-art methods by at least 4.65% with 81.0% average grasping success rate in real-world single-object environment and 75.3% grasping success rate in cluttered scenes. We also proposed the multi-modal multi-fingered grasping dataset generation method. Our multi-fingered hand grasping dataset outperforms previous datasets in scene diversity, modality diversity. The dataset, code and supplementary materials can be found at <https://sites.google.com/view/ffh-cluttered-grasping>.

I. INTRODUCTION

Utilizing a multi-fingered hand for robotic grasping enhances both ease and flexibility, primarily through the increased number of contact points available for interaction. Recent advancements in multi-fingered robotic grasping research [1]–[7] have focused on leveraging hand-object contact information to guide the generation of grasping strategies. By utilizing contact points and contact distance maps, respectively, UniGrasp [1] and GenDexGrasp [2] guide the grasp generation process, thereby enhancing the generalization of grasping strategies across different robotic hands. However, the contact points generated by UniGrasp [1] are sparse, limiting the diversity of the generated grasps. The contact distance maps lack semantic information, which leads to instability in the grasping samples generated under their guidance. To solve these limitations of contact information-guided grasp generation methods, we propose the CoSe-CVAE to generate contact semantic maps for assisting grasp generation.

In addition to contact information-guided grasp generation methods, recent advancements in multi-fingered hand grasping have enabled the grasp generation from visual data through deep learning methods [8]–[10], generation model [11], [12]. However, real-world scenarios are often cluttered, making grasp planning for multi-fingered hands

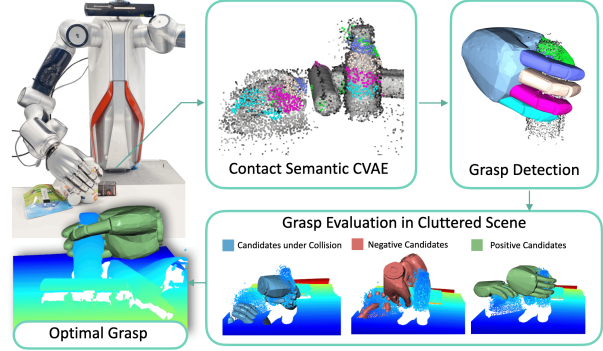


Fig. 1. Employing CoSe-CVAE, the contact semantic maps are derived from object point clouds. Grasp detection leverages contact prior information for estimating grasp poses. Subsequent grasp evaluation assesses both grasping qualities with collision awareness to identify the optimal grasp in cluttered settings. (Blue: grasp candidates colliding with the surroundings, Red: negative grasp candidates, Green: Positive grasp candidates.)

particularly challenging. Additionally, the high degrees of freedom in multi-fingered hands further complicate the generation and evaluation of collision-free, high-quality grasps. Despite numerous studies [8], [13]–[20] exploring the grasping in cluttered scenes using various end-effectors, their ability to reliably evaluate multi-fingered hand grasping in such environments remains limited. HGC-Net [8] remains unstable when evaluating grasps colliding with the surroundings. Moreover, these methods are often tailored to specific robotic hand designs, lacking the flexibility to generalize across different multi-fingered hands. To address mentioned limitations, we introduce a grasp evaluator to estimate grasp quality and collision probability, leveraging point cloud data from both the object and the robotic hand.

Our research introduces a multi-fingered hand grasping generation pipeline using contact semantic map in cluttered scenes. This pipeline includes the CoSe-CVAE, a grasp detection method and the grasp evaluation model. CoSe-CVAE is designed to generate contact semantic maps, where the semantic information indicates which fingers are in contact with the object. Furthermore, the grasp poses are estimated based on predicted contact semantic maps and optimal grasp is selected based on grasp qualities from grasp evaluation model. Our main contributions are as follows:

- 1) We propose a contact semantic conditional variational autoencoder network (CoSe-CVAE) that generates multi-fingered grasping contact semantic maps from object point clouds. CoSe-CVAE generates richer, more diverse contact point maps with semantic information, enabling more stable and reliable grasp

†Corresponding author. kaixin.bai@studium.uni-hamburg.de

¹TAMS (Technical Aspects of Multimodal Systems), Department of Informatics, Universität Hamburg, Hamburg, Germany, ²Agile Robots AG, Munich, Germany, ³Technical University of Munich, Munich, Germany.

TABLE I
COMPARISON OF MULTI-FINGERED ROBOTIC HAND GRASPING DATASETS.

Methods	Hand Type	Cluttered Scene	Grasp Quality	Evaluation Metric	Contact Distance	Contact Semantic	Affordance
ContactPose [21], GRAB [22]	Human	✗	✗	-	✓	✓	✗
DexYCB [23]	Human	✓	✗	-	✓	✗	✗
GanHand [24]	Human	✓	✗	-	✓	✗	✓
DDGC [11]	Robot	✓	✓	GraspIt! [25]	✗	✗	✗
Columbia Grasp Database [26]	Robot	✗	✓	GraspIt! [25]	✗	✗	✗
Fast-Grasp'D [27]	Robot	✗	✓	Trial-and-Error	✗	✗	✗
DexGraspNet [28]	Human&Robot	✗	✓	Trial-and-Error	✓	✗	✗
GenDexGrasp [2]	Robot	✗	✓	Trial-and-Error	✓	✗	✗
Ours	Robot	✓	✓	Trial-and-Error	✓	✓	✓

- generation guided by contact information.
- 2) We introduce a grasp evaluation network estimating grasp scores by analysing the partial scene point cloud and hand geometric features based on PointNet++ [29]. The network is capable of evaluating grasping in cluttered scenes for both known and unknown multi-fingered hands. Our method outperforms SOTA approaches [1], [2], [8] in average grasp success rate by at least 4.65%.
 - 3) We integrate a pipeline for generating a multi-modal multi-fingered grasping dataset in cluttered environments, based on DexGraspNet [28]. Its scene complexity and number of modalities surpass those of previous five-finger hand datasets.

II. RELATED WORK

A. Multi-fingered Robotic Hand Grasping in Cluttered Environments

Grasping in cluttered environments using multi-fingered robotic hands presents a significant challenge due to their high degrees of freedom and the complex collision dynamics with surrounding objects. Compared to two-jaw grippers, multi-fingered robotic hands can establish more contact points, allowing them to grasp more complex objects with enhanced dexterity. Although there has been extensive research [18], [30], [31] on grasping in cluttered environments with two-jaw gripper, studies on multi-fingered robotic hand grasping in such environments remain limited [8], [14], [15], [32]. Currently, datasets for multi-fingered robotic hand grasping in cluttered environments are severely limited. We provide an overview of existing multi-fingered hand grasping datasets and their available modalities, as summarized in Tab. I. However, there are no dataset that includes cluttered scenes while capturing all relevant multi-modal information. To date, no studies have utilized contact information to guide grasp generation in cluttered environments with multi-fingered robotic hands, and no corresponding datasets have been developed. To address this gap, we extended the existing grasp generation pipeline [28] to cluttered environments, producing contact semantic maps. Building on this, we propose a novel contact information-guided method for multi-fingered robotic hand grasp generation in cluttered scenes.

B. Contact Information-guided Grasping Generation

Hand-object representations are widely used in various domains: they are crucial for generating plausible hand poses [4]–[6], formulating generalized representations for

diverse end-effectors [1], [2], and bridging the gap between human and robotic hand representations [7], [33]. Various types of contact representations are employed, including contact touch code [33], contact distance or points [1], [3], [34], contact semantic map [21], [22]. UniGrasp [1] introduced a generalized model that sequentially generates contact points. Generative models, renowned for their diversity and generative capabilities, have been increasingly applied in the field of grasp generation. Notable examples include the application of CVAE [2], [35], [36] and diffusion model [37]. GenDexGrasp [2] employed a generative model to generate contact distance maps from object point clouds. However, these methods do not address how to generate contact semantic map from scene point cloud and generate stable multi-fingered hand grasps using contact semantic map in complex environments. Additionally, we found that grasps generated using contact distance maps lacked stability due to the absence of semantic information. To address these limitations, we propose a novel generative model, named CoSe-CVAE, which generates contact semantic maps from object point clouds and incorporates the grasp generation pipeline for cluttered environments.

C. Grasping Evaluation in Cluttered Scenes

Concerning collision-free grasp detection in cluttered environments, extensive research has been conducted on employing neural networks to predict collision-free grasp samples from visual data, particularly in the context of two-fingered grasping setups [8], [16]–[20], [30], [38]. Our previous work [30] developed a cable grasping neural network (CG-CNN) aiming at estimating grasp quality for cables in cluttered scenes, using implicit collision representations. However, multi-fingered hands, with their additional joints, pose greater challenges in learning implicit collision representations. Previous evaluators [39] were often designed for a specific robotic hand and lacked the ability to generalize across different hand types. To address this complexity and identify optimal grasp candidates in cluttered environments, we develop an unified grasp evaluation model that estimate grasp scores with collision awareness from partial scene point cloud and the point cloud of robotic hand, while being adaptable to various robotic hands.

III. PROBLEM STATEMENT AND METHODS

A. Problem Statement

In multi-fingered robotic hand grasping tasks within cluttered scenes, it's crucial to consider both hand grasp quality

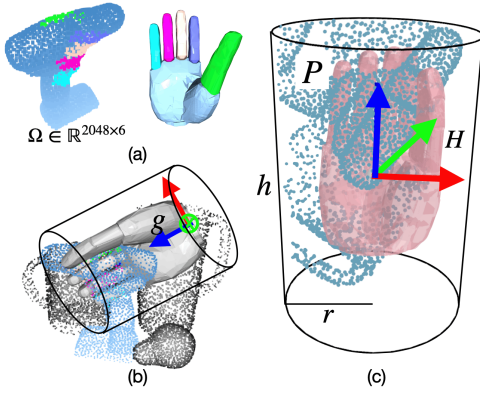


Fig. 2. (a) The CoSe-CVAE model predicts contact semantic maps based on the object’s point cloud, representing both the geometric and semantic information of contact points across different fingers. (b) Grasp candidate in cluttered scene. (c) The grasp evaluation network assesses grasp quality by utilizing partial scene point cloud surrounding the grasp sample P , along with the sampled point cloud of the multi-fingered hand H .

and the collision probability with the surrounding unstructured environment.

We define a robotic hand pose $g = [T, \Theta]$. T denotes hand wrist pose, Θ represents joint poses $(\theta_1, \theta_1, \dots, \theta_d)$. d denotes the number of degrees of freedom (DOF), corresponding to 15 DOF and 20 joints in the DLR-HIT II hand [40]. The dataset generation of multi-fingered robotic hand grasping is detailed in Sec. III-B.

We utilize contact semantic map $\Omega \in \mathbb{R}^{2048 \times (n+1)}$ with 2048 points to represent the contact points between n fingers of robotic hand and grasped object and points without contacts, as shown in Fig. 2 (a). Generative model CoSe-CVAE f is able to estimate N contact semantic maps from object point cloud O , as introduced in Sec. III-C. Grasp detection F is presented in Sec. III-D to estimate grasp candidates based on contact semantic maps. For estimating the optimal grasp candidate g_{optimal} from a cluttered scene’s point cloud, grasp evaluation network Ψ infers grasp qualities q from partial scene point cloud P and sampled hand point cloud H , as described in Sec. III-E. The partial scene point cloud is obtained through filtering the original scene points using a cylindrical region in the robotic hand’s frame, defined by a radius r and height h , as depicted in Fig. 2 (c). The optimal grasp pose g_{optimal} is selected based on these inferences. The pipeline is summarized in Eq. 1.

$$\begin{aligned}
 \bigcup_{i=0}^{N-1} g_i &= \bigcup_{i=0}^{N-1} F(f_i(O)) \\
 \bigcup_{i=0}^{N-1} q_i &= \bigcup_{i=0}^{N-1} \Psi(P_i, H_i) \\
 g_{\text{optimal}} &= \arg \max_g \bigcup_{i=0}^{N-1} q_i
 \end{aligned} \quad (1)$$

B. Multi-Modal Multi-fingered Hand Grasping Dataset Generation

To effectively address the complexities of multi-fingered robotic hand planning in intricate environments, we have

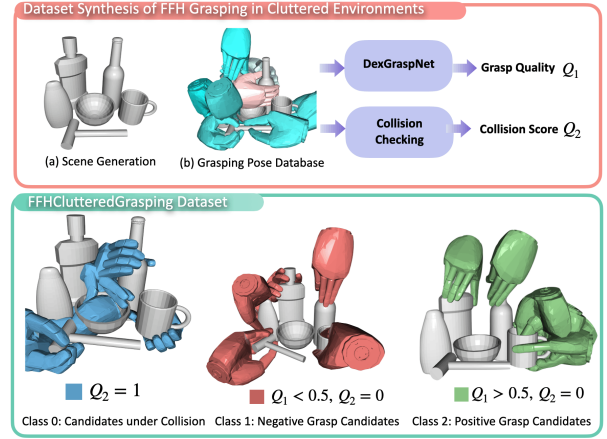


Fig. 3. Pipeline for generating multi-fingered robotic hand grasps in cluttered settings, involving scene generation, hand pose generation, collision checking, grasp quality validation, and dataset labeling with grasp quality and collision status. Grasping candidates under collision condition are plotted in blue. Unreliable grasp candidates, where $Q_1 < 0.5$, are highlighted in red, while reliable grasp candidates are marked in green.

developed a method for grasping synthesis. The algorithm pipeline is summarized in Alg. 1 and shown in Fig. 3.

Algorithm 1 Dataset Synthesis Algorithm

- 1: **Input:** Object database, Number of sampling grasp poses M , Number of objects in scene m
- 2: **Output:** Set of multi-fingered robotic hand grasping candidates with grasp pose g , grasp quality Q_1 , collision score Q_2 , contact semantic map Ω
- 3: **Procedure 1:** Estimate grasp pose g , grasp qualities Q_1 based on [28], contact distance map based on [2].
- 4: **Procedure 2:** Contact semantic mapping estimation as detailed in III-B.1
- 5: **Procedure 3:** Cluttered scene generation and collision evaluation
- 6: **repeat**
- 7: Build cluttered scene with m objects based on collision checking among objects [18].
- 8: Estimate collision state between j grasping candidates and corresponding surrounding objects to obtain collision scores $\bigcup_{j=0}^{M-1} Q_{2j}$. The collision score of j th candidate is denoted by Q_{2j} .
- 9: **until** Finish collision checking for all multi-fingered robotic grasping samples for cluttered scenes.

1) *Contact Semantic Map Estimation:* The contact semantic map is computed by estimating the nearest points on object surface to hand’s fingers. Coarse-estimated nearest points on object’s surface P_n is calculated based on aligned distance $\epsilon(\phi_{\text{finger}}, O)$ [2], normal vector n_o of object surface point and robotic hand surface point v_h , as formalized in Eq. 2. Each finger’s surface point is denoted by ϕ_{finger} and the object point cloud is represented using O . However, the nearest object point is located outside the object surface, when the normal vector n_o is not accurately predicted. To solve this problem, we filter out the nearest points on

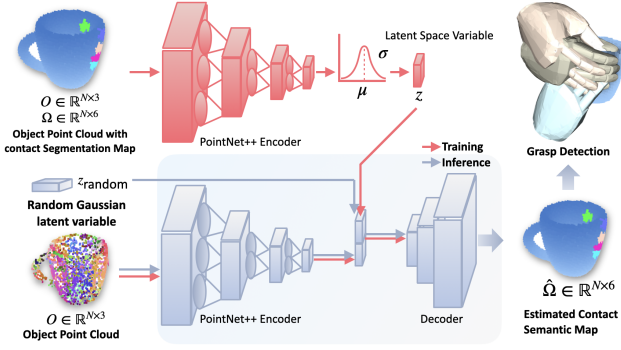


Fig. 4. Contact Semantic Map Generation and Grasping Detection.

the surface of the object according to distances between estimated nearest points and object surface points. The object point clouds with contact semantic labels are denoted by P_{contact} . This process is formalized as follows:

$$\begin{aligned}
 P_n &= \{v_h - \epsilon_{\min} n_o, \forall v_h \in \phi_{\text{finger}}\} \\
 P_{\text{contact}} &= \left\{ (p', L) \mid p' \in O, \exists p \in P_n \right. \\
 &\quad \left. \text{s.t. } \|p - p'\| < \tau \text{ and } L = l \right\}
 \end{aligned} \quad (2)$$

where, ϵ_{\min} denotes the aligned distance characterized by the smallest absolute value. τ signifies the threshold parameter. The semantic label L is denoted by the classification index of the fingers l , shown in Fig. 3 and is used to label the contact semantic categories of the object's point cloud. Consequently, contact semantic map $\Omega \in \mathbb{R}^{2048 \times (n+1)}$ is shown in Fig. 2 (a).

C. Contact Semantic CVAE

Given the point cloud data of objects, we employ a novel generative model, Contact Semantic Conditional Variational Autoencoder (CoSe-CVAE), to learn the network for predicting contact semantic maps, as shown in Fig. 4. In the encoder, the point cloud data O and contact semantic map Ω are processed through PointNet++ [29] to extract both global and local features. The features abstracted from data with contact semantic information are then utilized to predict the mean μ and variance σ , from which the latent space variable z is sampled from the data distribution. In the decoder, the latent space variable z and the input point cloud data O are utilized to initially predict the contact semantic maps $\hat{\Omega}$. The encoder and decoder parameters, φ and θ , are updated by maximizing the evidence lower bound (ELBO) of log-likelihood of $\log p_{\theta, \varphi}(\Omega \mid O)$, as follows:

$$\begin{aligned}
 \log p_{\theta, \varphi}(\Omega \mid O) &\geq \mathbb{E}_{z \sim Z} [\log p_{\varphi}(\Omega \mid z, O)] \\
 &\quad - \mathbb{KL} [p_{\theta}(z \mid \Omega, O) \parallel p_Z(z)] \\
 \mathbb{E}_{z \sim Z} [\log p_{\varphi}(\Omega \mid z, O)] &= \frac{1}{N_o} \sum_{i=0}^{N_o-1} \sum_{c=1}^C \omega_c \Omega_i^c \log(\hat{\Omega}_i^c)
 \end{aligned} \quad (3)$$

where, expectation of ELBO is estimated by weighted cross entropy loss of contact semantic map. Z represents standard normal distribution $\mathcal{N}(0, I)$. \mathbb{KL} denotes the Kullback-Leibler (KL) divergence. Ω and $\hat{\Omega}$ means the ground truth and estimated contact semantic map within a set of N_o samples and C classes. The class weight is denoted by ω .

D. Grasping Detection from Contact Semantic Maps

Using the generated contact semantic maps and the surface point clouds of each finger of the robotic hand, we utilize the correspondence point matching algorithm [41] to estimate the initial wrist pose. Inspired by GenDexGrasp [2] and UniGrasp [1], we optimize the wrist poses and finger tip positions by minimizing energy loss and the joint angles of the manipulator are calculated by differential inverse kinematics library mink [42]. The energy loss function e is formulated as follows:

$$e = \sum_{k=0}^{n-1} |\epsilon_s(v_k, \Omega_k)| \quad (4)$$

where, $\epsilon_s(v_k, \Omega_k)$ represents the signed distance from the fingertip position v_k of the k -th robotic finger to the contact points v_k , which are labeled with the semantic identifier k .

E. Grasp Evaluation Model

To identify optimal grasp in cluttered environments, we introduce an unified grasp evaluation model to quantify grasp quality, denoted as q . As illustrated in Fig. 5, our network architecture integrates inputs composed of hand surface points P and a partial scene point cloud H surrounding the target grasped object. The partial point cloud is captured relative to the hand's local frame. The point clouds are processed through two PointNet++ encoders, which extract latent spatial features of the hand and the scene point clouds. These latent features are concatenated and passed through a PointNet++ decoder to predict grasp classification scores. The classification includes three categories: Class 0 (grasp candidates under collision condition), Class 1 (negative grasp candidates), and Class 2 (positive grasp candidates). We employ a multi-class classification loss to guide the network's training. Specifically, we utilize the categorical cross-entropy loss, defined as:

$$\mathcal{L} = - \sum_{x=0}^{C-1} y_x \log(\hat{y}_x) \quad (5)$$

where C denotes the number of grasp categories, y_x is the ground truth label for class x , and \hat{y}_x represents the predicted probability for class x .

Among positive grasp candidates, the grasp candidate with higher scores are considered optimal.

IV. EXPERIMENT

A. Experimental Setup

We establish a platform equipped with Diana7 robot and DLR-HIT II Five-Finger hand [40] for conducting real-world experiments, as shown in Fig. 6 (a). The control of the robotic hand is achieved through joint impedance control. For capturing the scene's point cloud, we employ PhoXi 3D Scanner M camera. Grasped objects are shown in Fig. 6 (b) and (c).

During the experiments, the scene point cloud was segmented through instance segmentation and 6D pose estimation to extract object point clouds. For unknown objects, we utilized AnchorFormer [44] for object point cloud completion. After generating the optimal grasp using our pipeline, we employed the SE3 trajectory interpolation algorithm [45] to plan the robotic arm's trajectory.

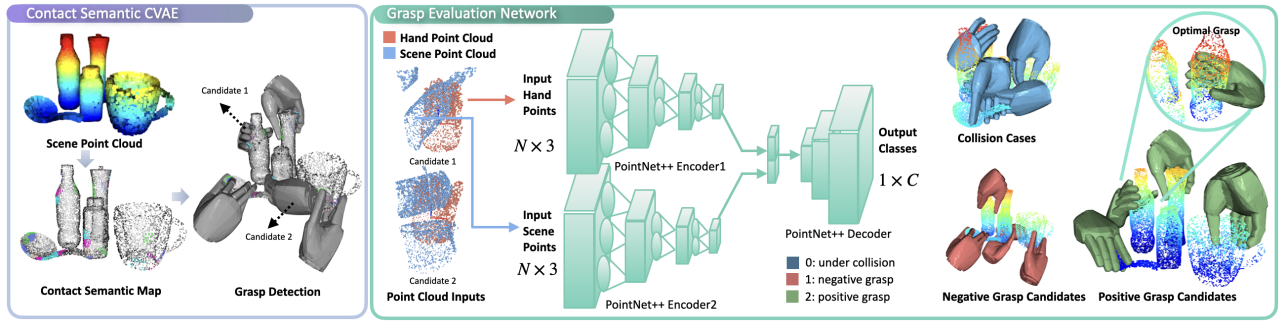


Fig. 5. Pipeline of multi-fingered robotic hand grasping network for grasping generation in cluttered environments. Firstly, contact semantic mappings are estimated from object point cloud employing CoSe-CVAE. Secondly, grasp detection method is utilized to generate hand postures from contact prior information. Finally, grasp evaluation network is used to estimated optimal grasp.

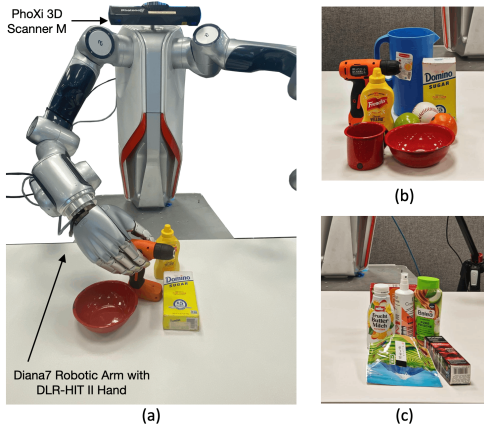


Fig. 6. (a) Experiment Setup. (b) Test objects from YCB-Video dataset [43] and (c) Household objects.

B. Multi-fingered Robotic Hand Grasping Dataset

Our dataset includes 1,521 household models from our previous work, as well as objects from the AffordPose dataset [46]. We generated over 2,000 scenes containing cluttered scene point clouds, collision scores, grasp quality, contact semantic maps, and grasp type information, contact distance map. We predict grasp types by voting based on the contact points and the object affordance label from [46], where the grasp type is determined by the affordance with the highest number of votes. The affordance labels include handle grasping, enveloping grasp, pouring, pressing, cutting, and twisting. In this work, we did not explore grasp type information in grasp generation. Dataset examples and grasp types are shown in the Fig. 3 and Fig. 7.

C. Model Training

We train CoSe-CVAE and grasp evaluation models using the cluttered scene point clouds, collision scores, grasp qualities, and contact semantic map data from the dataset. Adam optimizer is utilized with learning rates of $1e-4$ and $1e-3$ for training models on NVIDIA RTX 6000 Ada GPU. The radius r and height h of the cylinder region used for cropping part of the scene point cloud need to be adjusted according to the gripper dimensions. For DLR-HIT II hand, the radius r and height h are 0.1 meters and 0.3 meters, respectively.

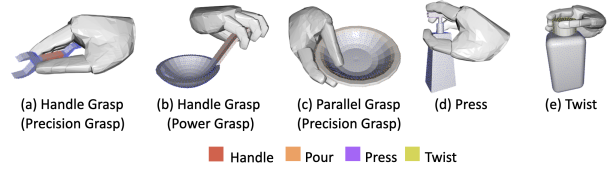


Fig. 7. Examples of grasping type considering object affordance maps and different manipulation poses.

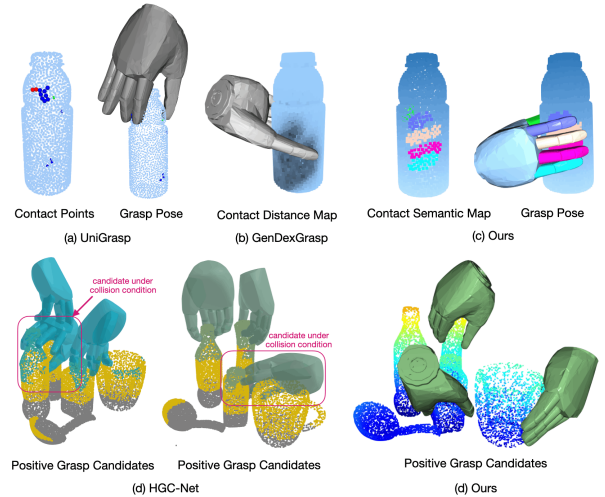


Fig. 8. Inference results for scene with single object and cluttered scenes. (a) Contact points and grasp candidate based on UniGrasp [1]. (b) Estimated Contact distance map and grasp pose from GenDexGrasp [2]. (c) Contact semantic map and grasp candidate from our methods. (d) Grasp candidates based on HGC-Net [8]. (e) Positive grasp candidates based on our methods.

D. Qualitative Study with SOTA methods

Qualitatively, we compare the grasp generation performance of our method with current contact information-guided grasp generation approaches, namely UniGrasp [1] and GenDexGrasp [2], as shown in Fig. 8. Additionally, we compare our method with the SOTA approach for grasp generation in cluttered environments, HGC-Net [8], to evaluate the performance in complex scenarios.

UniGrasp [1] predicts contact points one by one, while the CoSe-CVAE utilizes a generative model to predict all contact points simultaneously. As shown in Fig. 8 (a), the

contact points generated by UniGrasp are relatively sparse, and the method exhibits limited diversity in its outcomes. As the number of contact points increases, UniGrasp’s ability to account for the relationships between contact points diminishes, resulting in contact point predictions that fail to generate feasible grasp postures. CoSe-CVAE is more effective at considering the relationships between contact points, enabling it to generate diverse contact semantic maps.

GenDexGrasp [2] estimates contact distance map to guide optimization-based grasp generation, but it is prone to sub-optimal solutions in global optimization. As shown in Fig. 8 (b), the generated grasp samples do not match the predicted contact distance map. In contrast, the contact semantic map in our methods provides more accurate guidance for grasp generation, as shown in Fig. 8 (c).

The planning results for cluttered environments with unknown objects, using both our approach and the HGC-Net [8], are presented in Fig. 8. In real-world cluttered scenarios, HGC-Net demonstrates instability when handling objects under collision conditions, often resulting in failed grasps. As illustrated in the Fig. 8 (c) and (d), the optimal grasps generated by our model consistently outperform those of HGC-Net, delivering higher-quality results.

Incorporating contact semantic information into the grasping process significantly avoids local optimal candidate with opposite grasp pose, enhances the accuracy of the outcomes, leading to more effective grasp generation. Our grasp evaluation model is capable of assessing grasps in cluttered environments, consistently identifying the optimal grasp.

TABLE II

OUTCOMES OF REAL-WORLD GRASPING EXPERIMENTS

Method	Success Rate*(%)		
	household object	YCB object	Cluttered
GenDexGrasp [2]	62.7	58.7	-
UniGrasp [1]	71.3	70.7	-
HGC [8]	78.7	74.0	70.0
Ours	85.3	76.7	75.3

* Success rate is determined by executing 150 grasping attempts.

E. Quantitative Grasping Experiments

We conduct experiments in single-object grasping and grasping from cluttered environments, employing both our proposed method and baselines. Using our method, the grasping average success rate in single-object scenes reaches 81.0%, surpassing other baseline approaches [1], [2], [8]. Our grasp detection methods enhance the accuracy of grasping candidate selection. Additionally, our evaluation model substantially aids in filtering out unfeasible grasps for cluttered scenes. In grasping experiments from cluttered scenes, our method achieves a 75.3% success rate.

Most grasping failures are due to object slippage and ineffective force closure. Errors in joint angles during grasp generation cause slippage, while inaccuracies during the process prevent proper force closure. Failures often occur on object handles, where force-closure areas are limited.

F. Grasping Evaluation for Different Multi-fingered Robotic Hands

To verify the generalization capability of our grasp evaluation model across different robotic hands, we performed

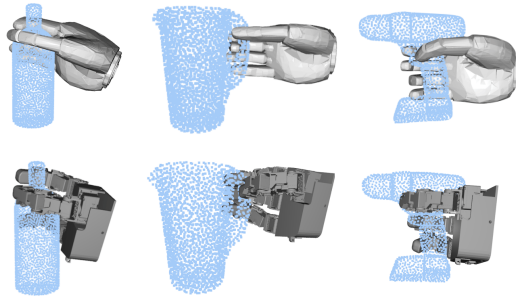


Fig. 9. Contact semantic map-guided grasp generation results using known DLR-HIT II hand and unknown LEAP hand.

real-world grasping experiments in cluttered scenes using both known hand, DLR-HIT II hand, and unknown robotic hand, four-fingered LEAP hand [47]. The results of the grasp generation with both DLR-HIT II hand and LEAP hand using same contact semantic maps are shown in the Fig 9. The average success rate of unknown hand achieves 74.0% in 50 grasping attempts.

V. CONCLUSIONS AND FUTURE WORK

We propose a novel method for multi-fingered grasp generation in cluttered environments, leveraging semantic contact information. First, the CoSe-CVAE model predicts diverse contact semantic maps between the hand and the object from the object’s point cloud. The grasp detection method then estimates grasp poses based on these semantic contact maps. Furthermore, our proposed grasp evaluation network utilizes both scene and robotic hand point clouds to predict grasp quality, selecting the optimal grasp in cluttered scenes. In this work, we also propose a pipeline for generating multi-modal multi-fingered robotic hand grasping dataset.

Qualitative real-world experiments demonstrate that our CoSe-CVAE model can reliably generate hand-object contact semantic information, significantly enhancing the stability of grasp generation based on contact information, outperforming SOTA methods [1], [2]. By incorporating the geometric characteristics of the robotic hand, the proposed grasp evaluation model can more effectively assess the grasp quality of multi-fingered hands in cluttered environments, outperforming [8]. Quantitative comparisons in real-world experiments further show that our method achieves a higher grasp success rate than these SOTA methods, with an average success rate of 81.0% in single-object scenarios and 75.3% in multi-object scenarios. Additionally, using an unknown robotic hand, we validate that our method achieves an average success rate of 74.0%.

In future work, we will explore how to leverage contact information to assist in complex and dexterous manipulations with robotic hands.

REFERENCES

- [1] L. Shao, F. Ferreira, M. Jorda, V. Nambiar, J. Luo, E. Solowjow, J. A. Ojea, O. Khatib, and J. Bohg, “Unigrasp: Learning a unified model to grasp with multifingered robotic hands,” *IEEE Robotics and Automation Letters*, vol. 5, no. 2, pp. 2286–2293, 2020.
- [2] P. Li, T. Liu, Y. Li, Y. Geng, Y. Zhu, Y. Yang, and S. Huang, “Gendex-grasp: Generalizable dexterous grasping,” in *2023 IEEE International Conference on Robotics and Automation (ICRA)*. IEEE, 2023, pp. 8068–8074.

- [3] S. Brahmabhatt, A. Handa, J. Hays, and D. Fox, "Contactgrasp: Functional multi-finger grasp synthesis from contact," in *2019 IEEE/RSJ International Conference on Intelligent Robots and Systems (IROS)*. IEEE, 2019, pp. 2386–2393.
- [4] H. Jiang, S. Liu, J. Wang, and X. Wang, "Hand-object contact consistency reasoning for human grasps generation," in *Proceedings of the IEEE/CVF International Conference on Computer Vision*, 2021, pp. 11 107–11 116.
- [5] L. Yang, X. Zhan, K. Li, W. Xu, J. Li, and C. Lu, "Cpf: Learning a contact potential field to model the hand-object interaction," in *Proceedings of the IEEE/CVF International Conference on Computer Vision*, 2021, pp. 11 097–11 106.
- [6] A. Wu, M. Guo, and C. K. Liu, "Learning diverse and physically feasible dexterous grasps with generative model and bilevel optimization," *arXiv preprint arXiv:2207.00195*, 2022.
- [7] H. B. Amor, O. Kroemer, U. Hillenbrand, G. Neumann, and J. Peters, "Generalization of human grasping for multi-fingered robot hands," in *2012 IEEE/RSJ International Conference on Intelligent Robots and Systems*. IEEE, 2012, pp. 2043–2050.
- [8] Y. Li, W. Wei, D. Li, P. Wang, W. Li, and J. Zhong, "Hgc-net: Deep anthropomorphic hand grasping in clutter," in *2022 International Conference on Robotics and Automation (ICRA)*. IEEE, 2022, pp. 714–720.
- [9] H. Duan, P. Wang, Y. Li, D. Li, and W. Wei, "Learning human-to-robot dexterous handovers for anthropomorphic hand," *IEEE Transactions on Cognitive and Developmental Systems*, vol. 15, no. 3, pp. 1224–1238, 2022.
- [10] M. Liu, Z. Pan, K. Xu, K. Ganguly, and D. Manocha, "Deep differentiable grasp planner for high-dof grippers," *arXiv preprint arXiv:2002.01530*, 2020.
- [11] J. Lundell, F. Verdoja, and V. Kyrki, "Ddgc: Generative deep dexterous grasping in clutter," *IEEE Robotics and Automation Letters*, vol. 6, no. 4, pp. 6899–6906, 2021.
- [12] J. Lundell, E. Corona, T. N. Le, F. Verdoja, P. Weinzaepfel, G. Rogez, F. Moreno-Noguer, and V. Kyrki, "Multi-fingan: Generative coarse-to-fine sampling of multi-finger grasps," in *2021 IEEE International Conference on Robotics and Automation (ICRA)*. IEEE, 2021, pp. 4495–4501.
- [13] H. Duan, Y. Li, D. Li, W. Wei, Y. Huang, and P. Wang, "Learning realistic and reasonable grasps for anthropomorphic hand in cluttered scenes," in *2024 IEEE International Conference on Robotics and Automation (ICRA)*. IEEE, 2024, pp. 1893–1899.
- [14] B. Wu, I. Akinola, and P. K. Allen, "Pixel-attentive policy gradient for multi-fingered grasping in cluttered scenes," in *2019 IEEE/RSJ international conference on intelligent robots and systems (IROS)*. IEEE, 2019, pp. 1789–1796.
- [15] M. Corsaro, S. Tellex, and G. Konidaris, "Learning to detect multi-modal grasps for dexterous grasping in dense clutter," in *2021 IEEE/RSJ International Conference on Intelligent Robots and Systems (IROS)*. IEEE, 2021, pp. 4647–4653.
- [16] Z. Li, S. Li, K. Han, X. Li, Y. Xiong, and Z. Xie, "Planning multi-fingered grasps with reachability awareness in unrestricted workspace," *Journal of Intelligent & Robotic Systems*, vol. 107, no. 3, p. 39, 2023.
- [17] W. Wei, Y. Luo, F. Li, G. Xu, J. Zhong, W. Li, and P. Wang, "Gpr: Grasp pose refinement network for cluttered scenes," in *2021 IEEE International Conference on Robotics and Automation (ICRA)*. IEEE, 2021, pp. 4295–4302.
- [18] M. Sundermeyer, A. Mousavian, R. Triebel, and D. Fox, "Contactgraspnet: Efficient 6-dof grasp generation in cluttered scenes," in *2021 IEEE International Conference on Robotics and Automation (ICRA)*. IEEE, 2021, pp. 13 438–13 444.
- [19] M. Breyer, J. J. Chung, L. Ott, R. Siegwart, and J. Nieto, "Volumetric grasping network: Real-time 6 dof grasp detection in clutter," in *Conference on Robot Learning*. PMLR, 2021, pp. 1602–1611.
- [20] C. Wang, H.-S. Fang, M. Gou, H. Fang, J. Gao, and C. Lu, "Graspnet discovery in cluttered scenes for fast and accurate grasp detection," in *Proceedings of the IEEE/CVF International Conference on Computer Vision*, 2021, pp. 15 964–15 973.
- [21] S. Brahmabhatt, C. Tang, C. D. Twigg, C. C. Kemp, and J. Hays, "Contactpose: A dataset of grasps with object contact and hand pose," in *Computer Vision—ECCV 2020: 16th European Conference, Glasgow, UK, August 23–28, 2020, Proceedings, Part XIII 16*. Springer, 2020, pp. 361–378.
- [22] O. Taheri, N. Ghorbani, M. J. Black, and D. Tzionas, "Grab: A dataset of whole-body human grasping of objects," in *Computer Vision—ECCV 2020: 16th European Conference, Glasgow, UK, August 23–28, 2020, Proceedings, Part IV 16*. Springer, 2020, pp. 581–600.
- [23] Y.-W. Chao, W. Yang, Y. Xiang, P. Molchanov, A. Handa, J. Tremblay, Y. S. Narang, K. Van Wyk, U. Iqbal, S. Birchfield *et al.*, "Dexycb: A benchmark for capturing hand grasping of objects," in *Proceedings of the IEEE/CVF Conference on Computer Vision and Pattern Recognition*, 2021, pp. 9044–9053.
- [24] E. Corona, A. Pumarola, G. Alenya, F. Moreno-Noguer, and G. Rogez, "Ganhand: Predicting human grasp affordances in multi-object scenes," in *Proceedings of the IEEE/CVF conference on computer vision and pattern recognition*, 2020, pp. 5031–5041.
- [25] A. T. Miller and P. K. Allen, "Graspi! a versatile simulator for robotic grasping," *IEEE Robotics & Automation Magazine*, vol. 11, no. 4, pp. 110–122, 2004.
- [26] C. Goldfeder, M. Ciocarlie, H. Dang, and P. K. Allen, "The columbia grasp database," in *2009 IEEE international conference on robotics and automation*. IEEE, 2009, pp. 1710–1716.
- [27] D. Turpin, T. Zhong, S. Zhang, G. Zhu, J. Liu, R. Singh, E. Heiden, M. Macklin, S. Tsogkas, S. Dickinson *et al.*, "Fast-grasp'd: Dexterous multi-finger grasp generation through differentiable simulation," *arXiv preprint arXiv:2306.08132*, 2023.
- [28] R. Wang, J. Zhang, J. Chen, Y. Xu, P. Li, T. Liu, and H. Wang, "Dexgraspnet: A large-scale robotic dexterous grasp dataset for general objects based on simulation," in *2023 IEEE International Conference on Robotics and Automation (ICRA)*. IEEE, 2023, pp. 11 359–11 366.
- [29] C. R. Qi, L. Yi, H. Su, and L. J. Guibas, "Pointnet++: Deep hierarchical feature learning on point sets in a metric space," *Advances in neural information processing systems*, vol. 30, 2017.
- [30] L. Zhang, K. Bai, Q. Li, Z. Chen, and J. Zhang, "A collision-aware cable grasping method in cluttered environment," *arXiv preprint arXiv:2402.14498*, 2024.
- [31] H. Liang, X. Ma, S. Li, M. Görner, S. Tang, B. Fang, F. Sun, and J. Zhang, "Pointnetgpd: Detecting grasp configurations from point sets," in *2019 International Conference on Robotics and Automation (ICRA)*. IEEE, 2019, pp. 3629–3635.
- [32] D. Berenson and S. S. Srinivasa, "Grasp synthesis in cluttered environments for dexterous hands," in *Humanoids 2008-8th IEEE-RAS International Conference on Humanoid Robots*. IEEE, 2008, pp. 189–196.
- [33] T. Zhu, R. Wu, X. Lin, and Y. Sun, "Toward human-like grasp: Dexterous grasping via semantic representation of object-hand," in *Proceedings of the IEEE/CVF International Conference on Computer Vision*, 2021, pp. 15 741–15 751.
- [34] Q. Liu, Y. Cui, Q. Ye, Z. Sun, H. Li, G. Li, L. Shao, and J. Chen, "Dexrepnet: Learning dexterous robotic grasping network with geometric and spatial hand-object representations," in *2023 IEEE/RSJ International Conference on Intelligent Robots and Systems (IROS)*. IEEE, 2023, pp. 3153–3160.
- [35] W. Wei, D. Li, P. Wang, Y. Li, W. Li, Y. Luo, and J. Zhong, "Dvvg: Deep variational grasp generation for dextrous manipulation," *IEEE Robotics and Automation Letters*, vol. 7, no. 2, pp. 1659–1666, 2022.
- [36] A. Mousavian, C. Eppner, and D. Fox, "6-dof graspnet: Variational grasp generation for object manipulation," in *Proceedings of the IEEE/CVF International Conference on Computer Vision*, 2019, pp. 2901–2910.
- [37] J. Urain, N. Funk, G. Chalvatzaki, and J. Peters, "Se (3)-diffusionfields: Learning cost functions for joint grasp and motion optimization through diffusion," *arXiv preprint arXiv:2209.03855*, 2022.
- [38] H.-S. Fang, C. Wang, M. Gou, and C. Lu, "Graspnet-1billion: A large-scale benchmark for general object grasping," in *Proceedings of the IEEE/CVF conference on computer vision and pattern recognition*, 2020, pp. 11 444–11 453.
- [39] V. Mayer, Q. Feng, J. Deng, Y. Shi, Z. Chen, and A. Knoll, "Ffhnet: Generating multi-fingered robotic grasps for unknown objects in real-time," in *2022 International Conference on Robotics and Automation (ICRA)*. IEEE, 2022, pp. 762–769.
- [40] Z. Chen, N. Y. Lii, T. Wimboeck, S. Fan, M. Jin, C. H. Borst, and H. Liu, "Experimental study on impedance control for the five-finger dexterous robot hand dlr-hit ii," in *2010 IEEE/RSJ International Conference on Intelligent Robots and Systems*. IEEE, 2010, pp. 5867–5874.
- [41] S. Rusinkiewicz and M. Levoy, "Efficient variants of the icp algorithm," in *Proceedings third international conference on 3-D digital imaging and modeling*. IEEE, 2001, pp. 145–152.
- [42] K. Zakka, "Mink," 2024. [Online]. Available: <https://github.com/kevinzakka/mink>
- [43] B. Calli, A. Walsman, A. Singh, S. Srinivasa, P. Abbeel, and A. M. Dollar, "Benchmarking in manipulation research: The ycb object and model set and benchmarking protocols," *arXiv preprint arXiv:1502.03143*, 2015.
- [44] Z. Chen, F. Long, Z. Qiu, T. Yao, W. Zhou, J. Luo, and T. Mei, "Anchorformer: Point cloud completion from discriminative nodes," in *Proceedings of the IEEE/CVF conference on computer vision and pattern recognition*, 2023, pp. 13 581–13 590.

- [45] W. Maddern, G. Pascoe, C. Linegar, and P. Newman, "1 Year, 1000km: The Oxford RobotCar Dataset," *The International Journal of Robotics Research (IJRR)*, vol. 36, no. 1, pp. 3–15, 2017. [Online]. Available: <http://dx.doi.org/10.1177/0278364916679498>
- [46] J. Jian, X. Liu, M. Li, R. Hu, and J. Liu, "Affordpose: A large-scale dataset of hand-object interactions with affordance-driven hand pose," in *Proceedings of the IEEE/CVF International Conference on Computer Vision*, 2023, pp. 14 713–14 724.
- [47] K. Shaw, A. Agarwal, and D. Pathak, "Leap hand: Low-cost, efficient, and anthropomorphic hand for robot learning," *arXiv preprint arXiv:2309.06440*, 2023.